Three-Dimensional Study of the Effect of Block Roughness Geometry on Inclined Drop

Rasoul Daneshfaraz*, Ehsan Aminvash**, Silvia Di Francesco***, Amir Najibi**, John Abraham****

Abstract:

The main purpose of this study is to provide a method to increase energy dissipation on an inclined drop. Therefore, three types of rough elements with cylindrical, triangular and bat-shaped geometries are used on the inclined slope in the relative critical depth range of 0.128 to 0.36 and the effect of the geometry of these elements is examined using Flow 3D software. The results showed demonstrate that the downstream relative depth obtained from the numerical analysis is in good agreement with the laboratory results. The application of rough elements on the inclined drop increased the downstream relative depth and also the relative energy dissipation. The application of rough elements on the sloping surface of the drop significantly reduced the downstream Froude number, so that the Froude number in all models ranging from 4.7~7.5 to 1.45~3.36 also decreased compared to the plain drop. Bat-shaped elements are structurally smaller in size, so the use of these elements, in addition to dissipating more energy, is also economically viable.

1. Introduction

In water supply network systems, erodible waterways, water treatment systems, and in cases where the slope is large, it is possible to use inclined drop in order to better control the flow energy. Drop structures convert the natural slope of the ground to the design slope, cause energy dissipation, a reduction of velocity, and an increase in water depth. Therefore, in order to dissipate downstream energy of flow, an energy dissipation structure can be employed. Turbulence and the formation of mixed water and air are effective ways to increase energy consumption. The use of roughness elements in the flow path is a known method for energy dissipation. These elements are placed in the flow path; they often have different geometries and arrangements to increase energy dissipation. The purpose of this study is to investigate the effect of roughness elements on rectangular inclined drops.

* Corresponding Author: Professor, Department of Civil Engineering, Faculty of Engineering, University of Maragheh, Maragheh, Iran. Email: daneshfaraz@yahoo.com
** M.sc Student, Department of Civil Engineering, University of Maragheh, Maragheh, East Azarbaijan, Iran.
*** Assistant Professor, Faculty of Engineering, Niccolò Cusano University, Rome, Italy.
**** Professor, School of Engineering, University of St. Thomas, St Paul, MN, USA.

The parameters focused on are, hydraulic performance of the inclined drop and energy dissipation.

The first research on downstream energy dissipation from inclined drops was conducted by Wagner [33], which was an investigation of energy dissipation on inclined drops of the Columbia river. More recently, Ohtsu & Yasuda [25] studied the parameters of B and D type hydraulic jumps on sloping surfaces with angles ranging from 8 to 60 degrees. They provided relationships for the ratio of conjugate depth and hydraulic jump length. Pagliara et al., [27] investigated the energy dissipation on rough ramps; their results showed a decrease in relative energy dissipation with an increase in relative critical depth. Ahmad et al., [3] investigated energy dissipation on rough ramps with fixed boards with three different mean diameters. The results displayed that for all three sizes of roughness, energy loss decreases with increasing relative critical depth.

Ghare et al., [18] designed a rough ramp with four different slopes to investigate their effect on energy dissipation. The findings demonstrate that with increasing relative critical depth, energy dissipation for all four slopes decreased. Katourani and Kashefipour [21] conducted a laboratory study of the effect of spacing and baffle size on energy dissipation for flow over inclined drops. They found that

energy loss increases with increasing baffle width and spacing. Pagliara and Palermo [28] investigated the effect of the stilling basin geometry on energy dissipation in the presence of a rough ramp. The results point out that with increasing relative critical depth, the flow energy loss decreases.

Norouzi et al., [24] investigated downstream energy dissipation for an inclined drop with a vertical screen. Their study established that with increasing relative critical depth, relative energy dissipation had a downward trend. Abbaspour et al., [1] conducted an experimental study of energy dissipation on an inclined drop roughened with natural materials. The outcome demonstrates that the energy dissipation in the rough drop is 10 to 32% higher than for the smooth inclined drop.

Extensive experimental and numerical research has been conducted in the field of hydraulic jumping, which is exemplified by the research that will now be discussed. Among these studies, Sharif and Rostami [30] investigated the effect of flow rupture on energy dissipation in composite buckets using FLOW 3D software. The results indicate that buckets with an angle of 20 degrees had the best performance and the greatest energy depreciation. Jamil and Khan [20] examined hydraulic jumps with a circular cross. By increasing the Froude number, the relative length of the hydraulic jump and the total energy dissipation increased. Daneshfaraz et al., [14] investigated flow through ogee and stepped spillways using Fluent and Adina software. The finite volume solution was found to be superior to the finite element method.

Nayebzadeh et al., [23] numerically investigated hydraulic characteristics of the vertical drop with screens and the gradual divergence of the wall. Their simulations were performed using the FLOW 3D software package. The results indicate that the simultaneous use of wall divergence and screens downstream of a drop increased energy dissipation. Researchers have also performed various studies on hydraulic jump and energy dissipation in different conditions of the channel led by VOF and CFD methods. Babaali et al., [4] numerically simulated hydraulic jumps in stilling basins with converging walls. They found that the hydraulic jump performance with a convergent wall stilling basin is superior to the model with a non-shrinking wall.

Castillo et al., [5] performed laboratory and numerical studies of a hydraulic jump with FLOW 3D and ANSYS software. The RNG turbulence model has shown better performance compared to other turbulence models.

Some other numerical studies on hydraulic jumps and spillways include:

Daneshfaraz and Ghaderi [10] completed a numerical study on the effect of reverse curvature of ogee spillway using Fluent software. The findings demonstrate by increasing the

radius of curvature of the spillway, the maximum pressure decreased significantly.

Daneshfaraz et al., [13] numerically investigated the flow on a sharp-crested spillway. They evaluated a number of turbulence models and found that the RNG (k-ε) model was superior.

Daneshfaraz et al., [6] conducted experimental and numerical studies of energy dissipation for a flow with a sudden contraction. The finding showed that as the constriction increases, the energy dissipation of the flow increases. Also, Ghaderi et al., [15] numerically investigated free and submersible hydraulic jumps in the presence of macroroughness. The results showed that the numerical model was fairly well able to simulate the free and submerged jump characteristics.

Daneshfaraz et al., [11] Performed a laboratory study of energy dissipation and relative downstream depth in simple gabion incline breakers. The results indicate that in both models, the critical relative depth increase reduced energy consumption and increased the downstream relative depth.

The use of rough blocks on an inclined drop is rarely found. One of these structures was built as a forty-step (chehel pelleh) structure in Ardabil. Ardabil is one of the cities of Iran where rectangular cubic blocks are installed on an inclined drop. No studies have been performed to quantify the energy dissipation or determine other parameters of interest (Fig. 1). Since cube-shaped blocks use a large volume of materials, in the present study, bat-shaped, cylindrical, and triangular elements are employed. These shapes require less material than cubic elements.

Since the upstream flow regime of the inclined drop is often subcritical and becomes critical at the edge of the slope, it becomes supercritical as the flow continues downstream. The destructive kinetic energy resulting from the supercritical flow causes the erosion of the wall and the bed of the channel, and additional structures are usually used to dissipate this energy. Therefore, in the present study, in order to dissipate this energy, rough elements with different geometries have been used on the sloping surface of the inclined drop and its numerical hydraulic parameters have been investigated using software Flow 3D. The use of these elements, in addition to increasing energy dissipation, provides a lot of oxygen to the water and makes the downstream regime subcritical. For this reason, the use of these elements can be a very good alternative to stilling basins.

2. Materials and Methods

2.1 Dimensional analysis

As displayed in Figure 2, the parameters relevant to the inclined drop with roughness elements are listed. Figure 2 also shows the depth measurement locations, where y_0 is the

place of measuring the upstream depth, y_b is the place of measuring the depth of the edge of the drop, and y_1 is the place of measuring the downstream of the inclined drop, and the depth of the downstream of the inclined drop is measured at a distance of $1.5 \Delta Z$ (Daneshfaraz et al., [12]).

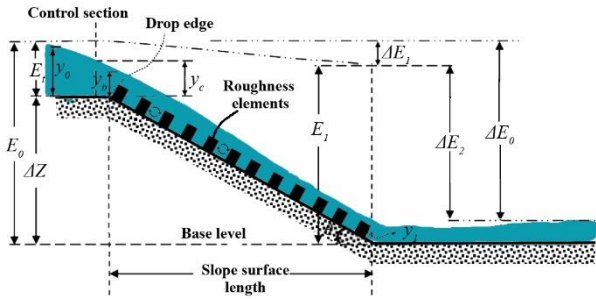**Fig. 1:** Model made in Ardabil, Iran

Fig. 2: Geometric and hydraulic parameters of an inclined drop equipped with roughness elements

$$\Delta E = f_1(\mu, \rho, g, q, \Delta Z, \theta, E_0, y_0, y_c, y_b, y_1, H, I) \quad (1)$$

Where: μ is dynamic viscosity [MLT^{-1}], ρ is density [ML^{-3}], g is acceleration gravity [LT^{-2}], q is discharge unit width [L^{2}T^{-1}], ΔZ is height of drop [L], θ is angle of the slope with the horizon surface [-], E_0 is upstream specific energy [L], y_0 is upstream depth [L], y_c is critical depth [L], y_b is edge of drop depth [L], y_1 is downstream depth [L], H is height of the rough elements [L] and I is percentage porosity of rough elements [-].

Using the Buckingham-Pi method and using parameters ρ, g and y_0 as iterative parameters, dimensional analysis is performed and the dependent parameters of relative energy dissipation are extracted as shown in Eqs. (2).

$$\frac{\Delta E}{E_0} = f_2(\text{Re}_0, Fr_0, \frac{\Delta Z}{y_0}, \theta, \frac{E_0}{y_0}, \frac{y_c}{y_0}, \frac{y_b}{y_0}, \frac{y_1}{y_0}, \frac{H}{y_0}, I) \quad (2)$$

Also, by simplifying and dividing some non-dimensional parameters, Eqs. (3) is presented as follows:

$$\frac{\Delta E}{E_0} = f_3(\text{Re}_0, Fr_0, \theta, \frac{\Delta Z}{y_0}, \frac{E_0}{\Delta Z}, \frac{y_c}{\Delta Z}, \frac{y_b}{y_c}, \frac{y_1}{\Delta Z}, \frac{H}{y_c}, I) \quad (3)$$

The flow is turbulent (the range of Reynolds number is mentioned in Table 1) and the angle and height of the drop are constant. Therefore, the parameters Re_0, θ, H/y_c and $E_0/\Delta Z$ were neglected (Daneshfaraz et al., [6, 7, 8, 9, 16]). As a result, the dimensionless parameters of relative energy dissipation, relative edge depth, and downstream relative depth of the inclined drop can be presented as Eqs. (4):

$$\frac{\Delta E}{E_0}, \frac{y_b}{y_c}, \frac{y_1}{\Delta Z} = f_4(\frac{y_c}{\Delta Z}) \quad (4)$$

Where: $\Delta E/E_0$ is relative energy dissipation [-], y_b/y_c is relative edge depth [-], $y_1/\Delta Z$ is relative downstream depth [-] and $y_c/\Delta Z$ is relative critical depth [-].

2.2 Evaluation criteria and equations

Two evaluation parameters, *RMSE*, R^2 and *KGE* have been used to validate the downstream relative depth from the numerical simulations with laboratory data. *RMSE* is the root mean square deviation and R^2 is the coefficient of determination and *KGE* is Kling-Gupta coefficient between the laboratory and numerical values. Optimally, the *RMSE* value goes to zero and the R^2 and *KGE* value approaches one. These two metrics are provided in Eqs. (5) and (6).

$$RMSE = \sqrt{\frac{\sum_{i=1}^{n}\left[\left(\frac{y_1}{\Delta Z}\right)_{Exp} - \left(\frac{y_1}{\Delta Z}\right)_{Num}\right]^2}{n}} \quad (5)$$

$$R^2 = \left(\frac{\sum_{i=1}^{N}((\frac{y_1}{\Delta Z})_{Exp} - \overline{(\frac{y_1}{\Delta Z})_{Exp}}) \times ((\frac{y_1}{\Delta Z})_{Num} - \overline{(\frac{y_1}{\Delta Z})_{Num}})^2}{\sqrt{\sum_{i=1}^{N}((\frac{y_1}{\Delta Z})_{Exp} - \overline{(\frac{y_1}{\Delta Z})_{Exp}})^2} \times \sqrt{\sum_{i=1}^{N}((\frac{y_1}{\Delta Z})_{Num} - \overline{(\frac{y_1}{\Delta Z})_{Num}})^2}}\right) \quad (6)$$

$$KGE = 1 - \sqrt{(R-1)^2 + (\beta-1)^2 + (\gamma-1)^2}$$
$$\beta = \frac{\overline{\text{Pr}e}}{\overline{Obs}}; \gamma = \frac{\sigma_{\text{Pr}e}/\overline{\text{Pr}e}}{\sigma_{Obs}/\overline{Obs}} \quad (7)$$

Also, the energy upstream (E_0) and downstream energy of the inclined drop (E_1) can be calculated as follows.

$$E_0 = \Delta Z + 1.5 y_c \quad (8)$$

$$E_1 = y_1 + \frac{q^2}{2gy_1^2} \quad (9)$$

2.3. Hydraulic model

FLOW 3D software is software that has been developed for solving complex computational fluid dynamics (CFD) issues. The governing equations are the Navier Stokes momentum conservation equations along with conservation of mass [10]. This software solves the coupled, nonlinear equations using the finite volume method calculated at each of a multitude of computational elements or grid cells. It is also a good alternative to physical models in solving fluid mechanics and hydrodynamics problems. This software has simplified the model and analysis of fluid behavior by using

numerical methods. One of the most important advantages of Flow 3D is the need for no additional modules in the solving problem process. This software performs 3D fluid flow analysis and has the ability to provide 1D, 2D and 3D outputs. The general form of the continuity and momentum equations is presented in Eqs. (10) and (11), respectively [14].

$$\frac{\partial U_i}{\partial x_j} = 0 \tag{10}$$

$$\frac{\delta U_i}{\delta t_i} + \rho U_i \frac{\partial U_i}{\partial x_i} - \frac{\partial P}{\partial x_i} + \frac{\partial}{\partial x_i}(\mu \frac{\partial U_i}{\partial x_j} - \rho u_j' u_i') + \rho g_i \tag{11}$$

Here, U_i and u_i' are the mean and fluctuating velocities, respectively in the direction xi. Tensor nomenclature is used so that $x_i = (x, y, z)$, $U_i = (U, V, W)$, $u_i' = (u', v', w')$. The symbols ρ, μ, P and g_i are density, dynamic viscosity, pressure, and gravitational acceleration, respectively. The instantaneous velocity can be obtained by $u_i = U_i + u_i'$ in all three directions. The RNG model is a two-equations model which accounts for turbulence. It is expressed as:

$$\frac{\partial}{\partial t}(\rho k) + \frac{\partial(\rho k u_i)}{\partial x_i} = \frac{\partial}{\partial x_j}(\alpha_k \mu_{eff} \frac{\partial k}{\partial x_j}) + G_k + G_b$$
$$- \rho \varepsilon - Y_M + S_k \tag{12}$$

$$\frac{\partial}{\partial t}(\rho \varepsilon) + \frac{\partial(\rho \varepsilon u_i)}{\partial x_i} = \frac{\partial}{\partial x_j}(\alpha_s \mu_{eff} \frac{\partial k}{\partial x_j}) + C_{1s} - \frac{\varepsilon}{k}(G_k + G_{3s} G_b)$$
$$+ C_{2\varepsilon} \rho \frac{\varepsilon^2}{k} - R_\varepsilon + S_\varepsilon \tag{13}$$

In these equations, k is the turbulent kinetic energy; ε is the turbulence dissipation rate; G_k is the production of turbulent kinetic energy due to the velocity gradient; G_b is turbulent kinetic energy production from buoyancy, and Y_M is turbulence dilation oscillation distribution [33], [22]. In the above equations, $\alpha_k = \alpha_s = 1.39$, $C_{1S} = 1.42$ and $C_{2S} = 1.6$ are model constants. The terms S_k and S_ε are sources terms for k and ε, respectively. The turbulent viscosity is added to the molecular viscosity to obtain, μ_{eff}, effective viscosity. The volume of Fluid (VOF) method consists of three main components: fluid ratio function, VOF transport equation solution, and boundary conditions at the free surface. The VOF transport equation is expressed by [15]:

$$\frac{\partial F}{\partial t} + \frac{1}{V_F}\left[\frac{\partial(FA_x u)}{\partial x} + \frac{\partial(FA_y v)}{\partial y} + \frac{\partial(FA_z w)}{\partial z} \right] = 0 \tag{14}$$

In the above equations, A is the average ratio of flow area along x, y and z directions; u, v and w are average velocities along x, y and z; and F is the fluid ratio function which takes on values between 0 and 1.

Turbulence simulation in FLOW 3D software is performed using turbulence model, namely:
I: Large Eddy Simulation model (LES)
II: k-ε equation model
III: Renormalized model group (RNG)
IV: The Prandtl mixing length

V: A turbulence kinetic energy equation

In the present study, from turbulence models RNG, k-ε and k-ω, model RNG was selected to simulate other models of this research. According to Table 1, by examining the results obtained from the simulation of the above turbulence models, it was observed that the correlation coefficient (R^2), the root means square error (RMSE) and the Kling-Gupta Efficiency (KGE) obtained from the turbulence model RNG have more appropriate values than other models.

Also, the reason for using this turbulence model is the ability to simulate a flow with a high number of meshes, good performance in simulating flow separation zones, better results against strain and sudden curvature of flow lines, and also selected according to previous numerical studies [2]; [16]; [19]; [26]; [29]; [31]; and [32].

Table. 1: Comparing experimental and numerical downstream relative depth in turbulence models

Turbulence models	Evaluation criteria		
	R^2	RMSE	KGE
RNG	**0.995**	**0.00371**	**0.995**
k-ε	0.989	0.051	0.955
k-ω	0.975	0.059	0.953

2.4. Simulation specification and solution field network

In the present study, in order to numerically simulate the effect of rough elements on the incline, a zigzag arrangement of roughness elements that occupied 15% of the flow area (a porosity of 15%) were used. There were three types of rough elements (cylindrical, triangular and bat-shaped geometries). The height of the elements was 1.5 cm. The height of the drop was 15 cm, making an angle of 26.56 degrees with the surface of the laboratory flume.

A total of 27 simulations were completed to account for the various roughness elements. Figure 3 shows a three-dimensional view of roughness elements located on the sloping surface of the inclined drop. A laboratory flume of 5 m long, 45 cm high and 30 cm wide from the hydraulic laboratory of University of Maragheh in Iran, was used for validating experiments. Rotameters with an error of ± 2% and a point gauge with an error of ±1 mm were used to measure the flow rate and depth, respectively. The downstream relative depth was used for validation.

The boundary conditions shown in Fig. 4 are as follows:
I: The inflow boundary = Volume Flow Rate
II: The outflow boundary = Outflow
III: The bottom and sides = Wall
IV: The top boundary = Symmetry

Table 2 shows the range of measured variables and Figure 4 shows the geometric characteristics of the inclined drop with boundary conditions in the presence of the bat-shaped

roughness element. Models M1, M2 and M3 represent bat-shaped, cylindrical and triangular blocks, respectively.
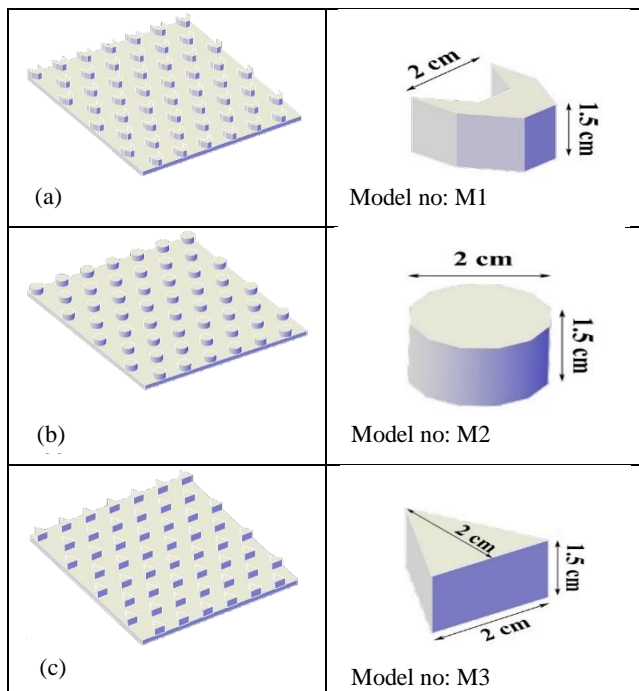

Fig. 3: Views of the incline with (a) Bat-shaped, (b) Cylindrical, (c) Triangular roughness elements

Table. 2: Range of measured variables

Model	Q (L/s)	y_1 (mm)	Fr_1	$Re_0 (\times 10^3)$
Smooth surface	2.5~11.7	5~19	4.69~7.5	32~138
M1	2.5~11.7	11~29.5	1.45~3.36	16~178
M2	2.5~11.7	17~27.5	1.56~3.0	39~145
M3	2.5~11.7	8.9~25.5	2.9~6	49~153
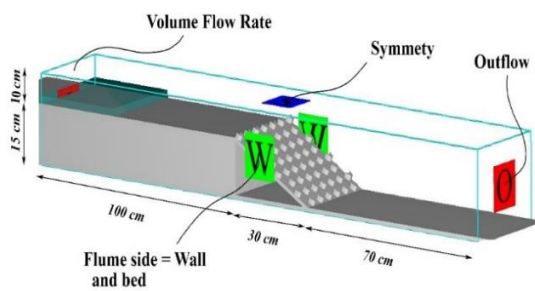
Fig. 4: Geometric profile of inclined drop and boundary conditions with the bat-shape roughness element

3. Results and Discussions

3.1. Solution stability

Collision of the flow with the roughness elements and the formation of two-phase flow with turbulence was created by the arrangement of the elements. The duration of the simulation was 15 seconds and the time step was 0.09 seconds. Time averaging of flow characteristics were obtained over a 10-second period. The reason for this is that

the flow is in a steady state in the 10th second and the data retrieval interval is done in terms of time from the 8th to the 12th second. In other words, data collection was done at different times 2 seconds before and 2 seconds after the steady state of the flow. As can be seen in Table 3, with computational element sizes of 0.0028 m the resulting RMSE and R^2 values were 0.00371 and 0.996, respectively. Fig 5 shows RMSE values with the cell size. The mesh used for the simulation is emboldened in Table 2.

Table. 3: Mesh sensitivity analysis for the present study

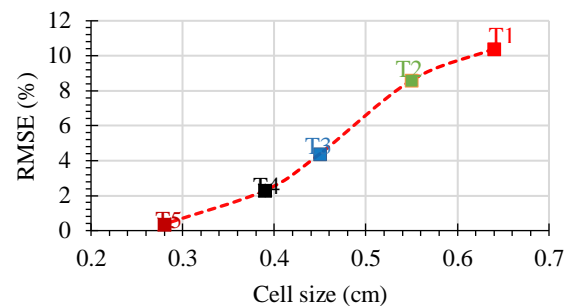| Test no.	Turbulence model	Cell size (cm)	Total number of cells	RMSE	R^2
T1	RNG	0.64	485,463	0.104	0.640
T2	RNG	0.55	760,760	0.086	0.776
T3	RNG	0.45	1,398,156	0.044	0.802
T4	RNG	0.39	2,133,054	0.023	0.886
T5	**RNG**	**0.28**	**5,729,850**	**0.00371**	**0.996**

Fig. 5: Variation of the RMSE varying cell size

3.2. Validation

Validation was performed by comparing laboratory measurements of the present study on a smooth inclined drop and output data obtained from FLOW 3D software. The relative downstream depths were compared and the results are shown in Figure 6. The simulated values of the downstream relative depth have root mean square error, and coefficient of determination of 0.00371 and 0.9958 for RNG; 0.051 and 0.989 for k-ε and 0.059 and 0.9753 for k-ω, respectively. This excellent agreement indicates the performance of the model performed.
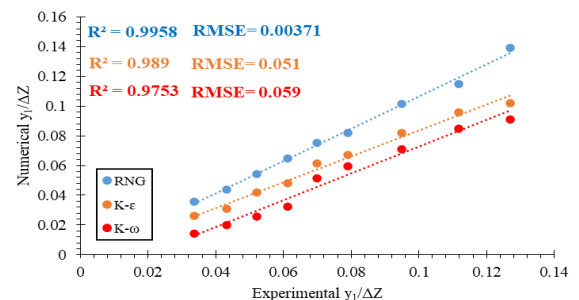

Fig. 6: Numerical and laboratory comparison of the downstream relative depth

3.3. Longitudinal flow profile

The longitudinal profile of the flow on a smooth inclined drop and a drop containing roughness elements on the slope is shown in Fig. 7. For the case with roughness elements, they are installed on a 15cm drop slope that has an angle of 26.56 degrees and a flowrate of 5 Lit/second. After the flow reaches the edge of the slope, it collides with the roughness elements and causes a two-phase flow. For the bat-shaped elements, a reverse flow occurs and passes through its sides. It is also observed that the presence of roughness elements on the inclined drop structure increases the downstream depth of the drop.
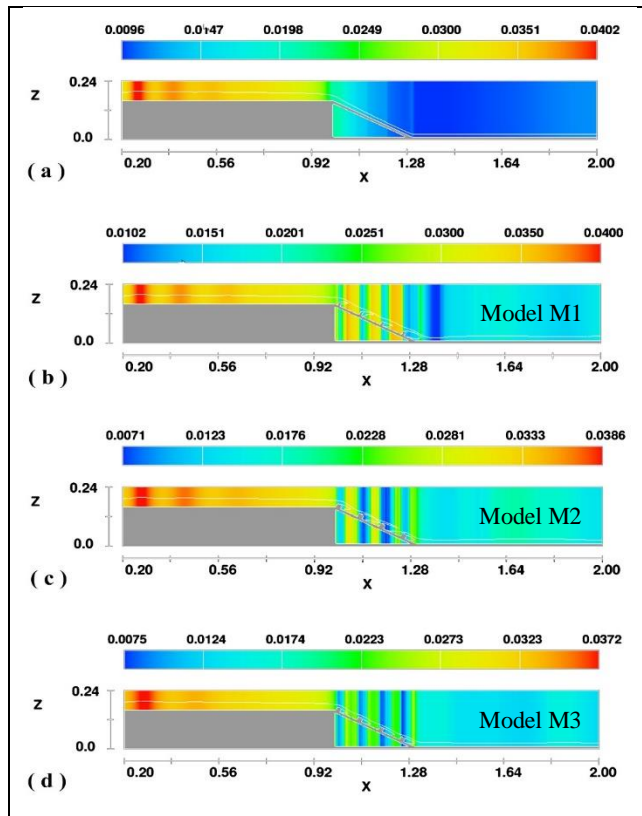

Fig. 7: Flow profile on inclined drop in discharge of 5 L/s: (a) Without roughness elements; (b) Bat-shaped roughness element; (c) Cylindrical roughness element; (d) Triangular roughness element

3.4. Relative edge depth

The relative depth of the edge can be a used for measuring the flow; Fig. 8 shows the changes in the relative depth of the edge versus the relative critical depth. According to Figure 8, the relative depth of the edge on the sloping surface roughened by the bat-shaped elements increases the drop's downstream depth with a greater slope and then assumes an almost constant value. The reason for this is that the flow depth with lower discharge is low. With the collision of the flow onto the first row of roughness, the flow depth increases and the flow falls down from the elements and passes through the obstacles as a non-submerged flow. As the flow rate increases, especially at flow rates of 5.8

Lit/second and above, the fluid passes over the obstacles in the form of a submerged flow and falls downstream. Triangular roughness elements behave similarly to bat-shaped elements at high discharges. As can be deduced from the figure, the cylindrical elements have the greatest relative depth of the edge. This is because when the flow strikes the cross section of the cylindrical element, the backwater profile increases by a relatively large amount. In addition to the contact of the flow with these elements, some of the flow moves downstream and another amount of it returns upstream. The physics of cylindrical elements is such that at the very beginning of the flow from the drop, it causes obstruction and this factor increases the relative depth of the edge. Also, because there is some obstruction in all elements, the relative depth of the edge in all models is greater than the depth of the edge of a simple inclined drop. The relative depth of the edge in the use of the cylindrical element that has the highest value increases the relative depth of the edge by 25% compared to a simple inclined drop. Fig. 9 shows the non-submerged and submerged flow for bat-shaped rough elements, as well as the flow striking and passing over the elements. The maximum relative depth of the edge occurs with the cylindrical elements because when the flow strikes this element shape, the backwater profile at the drop edge increases the depth of the edge.
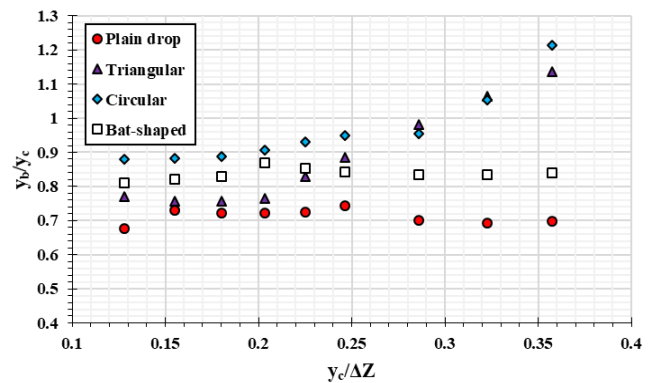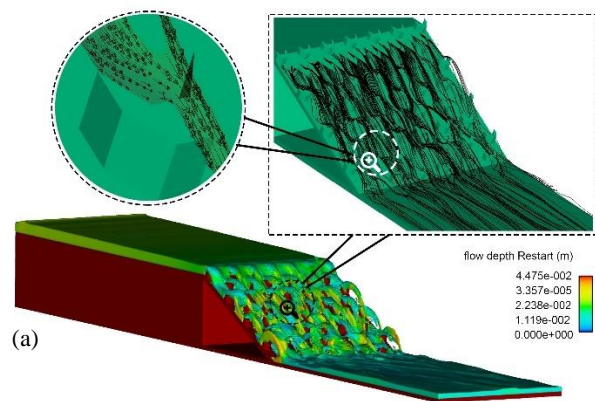

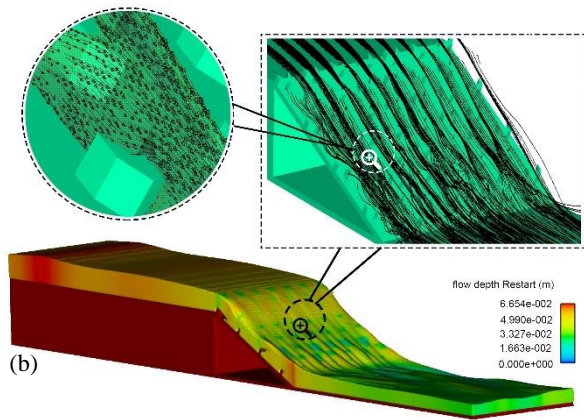**Fig. 8:** Relative edge depth versus the relative critical depth

(a)

Fig. 9: Flow on the inclined drop with bat-shaped elements: (a) Non-submerged flow; (b) Submerged flow

3.5. Downstream Relative depth

According to the dimensional analysis, Figure (10) shows the changes in the relative depth of the downstream based on the relative critical depth. According to Figure (10), it can be seen that with increasing relative critical depth, the downstream relative depth increases for all models.
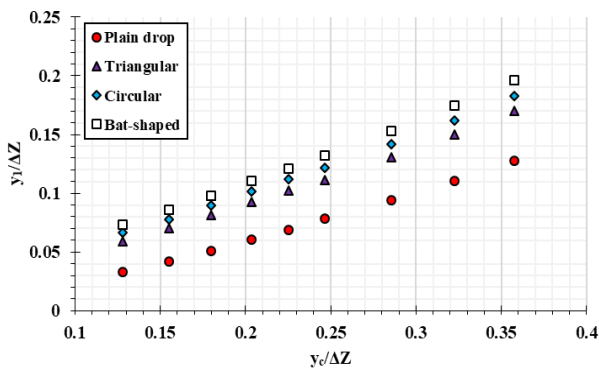

Fig. 10: Relative downstream depth versus the relative critical depth

The inclined drop equipped with the bat-shaped roughness element and the plain drop have the maximum and minimum downstream relative depth, respectively. Due to the fact that the flow on the plain drop is without mixing water and air interference, the relative depth of the downstream is less than the drops equipped with roughness. Rough elements on the sloping surface of the inclined drop used by dissipating energy through the structure itself, create hydraulic jumps and interfere with the air by creating turbulence and disturbing the flow lines through the interference of the air as the current passes through. Rough elements lead to an increase in the downstream relative depth. Among the rough elements used, the bat-shaped element, due to its unique geometry, increases the mixing water and air interference as much as possible, which leads to a further increase in the relative depth of the downstream.

3.5. Relative energy dissipation

Figure 11 shows the changes in relative energy dissipation in terms of the relative critical depth. It is inferred from Figure 11 that for all four models, by increasing the relative critical depth, the relative energy dissipation decreases. The highest and lowest energy dissipation belong to the inclined drop equipped with the bat-shaped roughness element and the smooth inclined drop, respectively. This is because as the inlet flow rate increases for all four models, the relative downstream depth increases. Due to the fact that the bat-shaped roughness element has a hollow space, by colliding the flow with this element, a backwater profile is created, which also causes energy dissipation. On the other hand, the formation of two-phase flow on the drop structure leads to an increase in shallow depth and also reduces the relative energy dissipation. Inclined drops equipped with triangular, cylindrical and bat-shaped roughness elements dissipate 65, 76, and 85% of the destructive energy of the flow, respectively. These exceed the dissipation that occurs with the smooth drop. Comparison of laboratory data from the smooth drop of Moradi-Sabzkoohi et al. (2011), which has a similar drop height and angle is also provided in the figure.
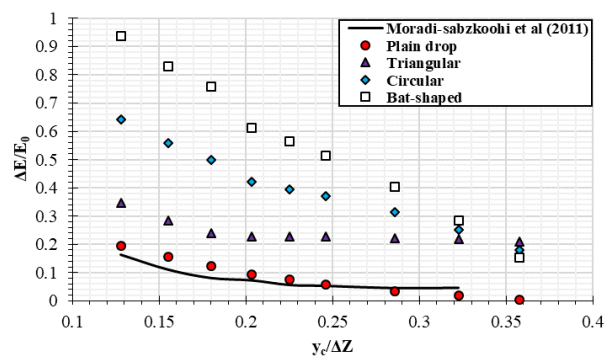

Fig. 11: Relative downstream depth versus the relative critical depth

4. Conclusions

In the current study, the effect of roughness element geometry on inclined drop hydraulic parameters using three types of roughness elements with triangular, cylindrical and bat-shaped geometries at one height, one angle, density of 15% and zigzag arrangement with FLOW-3D software was evaluated. VOF method was used to simulate free surface flow and initially three turbulence models RNG, k-ε and k-ω were used for validation, and after examining them, RNG method was used to simulate other models. the results demonstrated that:

1- The downstream relative depth of the smooth inclined drop obtained from the numerical results has a very good correlation with the laboratory data and the relative edge

depth in the inclined drop equipped with the cylindrical element had the highest value.

2- The downstream relative depth had an upward trend with the increase of the critical relative depth, so that the inclined drop equipped with the bat-shaped element and the smooth inclined drop have the highest and lowest downstream relative depth, respectively.

3- Relative energy dissipation decreases with increasing relative critical depth due to increasing downstream depth. In the meantime, the highest energy dissipation is related to the inclined drop equipped with a bat-shaped element and the lowest energy dissipation is related to the smooth drop. The drop equipped with triangular, cylindrical and bat-shaped rough elements, dissipates 65, 76 and 85% of the flow energy more than the smooth drop, respectively.

4- The application of rough elements on the sloping surface of the drop has significantly reduced the downstream Froude number so that the Froude number in all models ranging from 4.7~7.5 to 1.45~3.36 has decreased compared to the smooth drop. Also, due to the volume of bat-shaped roughness, which has a smaller volume than other elements, it is economical to use this type of roughness.

Acknowledgements:

References:

[1] Abbaspour, A., Shiravani, P., and Hosseinzadeh dalir, A., "Experimental study of the energy dissipation on the rough ramps", ISH journal of hydraulic engineering, 2019, p. 1-9.

[2] Abraham, J.P., Sparrow, E.M., Gorman, J.M., Zhao, Y., and Minkowycz, W.J., "Application of an Intermittency model for laminar, transitional, and turbulent internal flows", Journal of Fluids Engineering, vol. 141, 2019, paper no. 071204.

[3] Ahmad, Z., Petappa, N.M., and Westrich, B., "Energy dissipation on block ramps with staggered boulders", Journal of hydraulic engineering, vol. 135(6), 2009, p. 522-526.

[4] Babaali, H.R., Shamsai, A., and Vosoughifar, H.R., "Computational modeling of the hydraulic jump in the stilling basin with convergence walls using CFD codes", Arabian Journal for Science and Engineering, vol. 40(2), 2014, p. 381-395.

[5] Castillo, L.G., Carrillo, J.M., and Cacía, J.T., "Numerical simulations and laboratory measurements in hydraulic jumps", International conference on hydroinformatics. (2014, August) New York city.

[6] Daneshfaraz, R., Aminvash, E., Esmaeli, R., Sadeghfam, S., and Abraham, J., "Experimental and numerical investigation for energy dissipation of supercritical flow in sudden contractions", Journal of groundwater science and engineering, vol. 8(4), 2020a, p. 396-406.

[7] Daneshfaraz, R., Aminvash, E., Ghaderi, A., Kuriqi, A., and Abraham, J., "Three-dimensional investigation of hydraulic

properties of vertical drop in the presence of step and grid dissipators", Symmetry, vol. 13 (5), 2021a, p. 895.

[8] Daneshfaraz, R., Aminvash, E., Ghaderi, A., Abraham, J., and Bagherzadeh, M., "SVM performance for predicting the effect of horizontal screen diameters on the hydraulic parameters of a vertical drop", Applied sciences, vol. 11 (9), 2021b, p. 4238.

[9] Daneshfaraz, R., Bagherzadeh, M., Esmaeeli, R., Norouzi, R., and Abraham, J. "Study of the performance of support vector machine for predicting vertical drop hydraulic parameters in the presence of dual horizontal screens", Water supply, vol 21(1), 2021c, p. 217-231.

[10] Daneshfaraz, R., and Ghaderi, A., "Numerical investigation of inverse curvature ogee spillways", Civil engineering journal, vol. 3(11), 2017, p. 1146-1156.

[11] Daneshfaraz, R., Majedi Asl, M., and Bagherzadeh, M., "Experimental Investigation of the Energy Dissipation and the Downstream Relative Depth of Pool in the Sloped Gabion Drop and the Sloped simple Drop", AUT Journal of Civil Engineering, 2020b (In persian).

[12] Daneshfaraz, R., Majedi Asl, M., Bazyar, A., Abraham, J., Norouzi, R., "The laboratory study of energy dissipation in inclined drops equipped with a screen", Journal of Applied Water Engineering and Research, 2020c, p. 1-10.

[13] Daneshfaraz, R., Minaei, O., Abraham, J., Dadashi, S., and Ghaderi, A., "3-D Numerical simulation of water flow over a broad-crested weir with openings", ISH Journal of Hydraulic Engineering, 2019, p.1-9.

[14] Daneshfaraz, R., Sadeghfam, S., and Kashani, M., "Numerical simulation of flow over stepped spillways", Research in civil engineering and environmental engineering, vol. 2(4), 2014, p. 190-198.

[15] Ghaderi, A., Abbasi, S., Abraham, J., and Azamathulla, H.M., "Efficiency of trapezoidal labyrinth shaped stepped spillways", Flow measurement and instrumentation, vol. 72, 2020a.

[16] Ghaderi, A., Daneshfaraz, R., Dasineh, M., and Di Francesco, S., "Energy dissipation and hydraulics of flow over trapezoidal-triangular labyrinth weirs", Water, vol. 12(7), 2020b, p. 1-18.

[17] Ghaderi, A., Daneshfaraz, R., Torabi, M., Abraham, and Azamathulla, H.M. "Experimental investigation on effective scouring parameters downstream from stepped spillways", Water supply, vol. 20(4), 2020c, p. 1-11.

[18] Ghare, A.D., Ingle, R.N., Porey, P.D., and Gokhale, S.S. "Block ramp design for efficient energy dissipation", Journal of energy dissipation, vol. 136(1), 2010, p. 1-5.

[19] Gorman, J.M., Sparrow, E.M., Smith, C.J., Ghoash, A., Abraham, J.P., Daneshfaraz, R., Rezezadeh, J., "In-bend pressure drop and post-bend heat transfer for a bend with partial blockage at its inlet", Numerical Heat Transfer A, vol, 73, 2018, p. 743-767.

[20] Jamil, M., and Khan, S.A., "Theorical study of hydraulic jump in circular channel section", ISH journal of hydraulic engineering, vol. 16(1), 2010, p. 1-10.

[21] Katourani, S., and Kashefipour, S.M., "Effect of the geometric characteristics of baffle on hydraulic flow condition in baffled apron drop", Irrigation sciences and engineering, vol. 37(2), 2012, p. 51-59.

[22] Lai, Y.G., and Wu, K.A., "Three-dimensional flow and sediment transport model for free surface open channel flow on unstructured flexible meshes", Fluids, vol. 4(1), 2019, p. 1-19.

[23] Nayebzadeh, B., Lotfollahi yaghin, M.A., and Daneshfaraz, R., "Numerical investigation of hydraulic characteristics of vertical drops with screens and gradually wall expanding", Amirkabir journal of civil engineering, 2020 (In Persian).

[24] Nurouzi, R., Daneshfaraz, R., and Bazyar, A., "The study of energy dissipation due to the use of vertical screen in the downstream of inclined drop by adaptive Neuro-Fuzzy inference system (ANFIS)", AUT journal of civil engineering, 2019, (In Persian).

[25] Ohtsu, I., and Yasuda, Y., "Hydraulic jump in sloping channel", Journal of hydraulic engineering, vol. 117(7), 1991, p. 905-921.

[26] Olsen, L., Abraham, J.P., Cheng, L.K., Gorman, J.M., and Sparrow, E.M., "Summary of forced-convection fluid flow and heat transfer for square cylinders of different aspect ratios ranging from the cube to a two-dimensional cylinder", Advances in Heat Transfer, Vol. 51, 2019, p. 351-457.

[27] Pagliara, S., Das, R., and Palermo, M., "Energy dissipation on submerged block ramps", Journal of irrigation and drainage engineering, vol. 134(4), 2008, p.527-532.

[28] Pagliara, S., and Palermo, M., "Effect of stilling basin geometry on the dissipative process in the presence of block ramps", Journal of irrigation and drainage engineering, vol. 138(11), 2012, p. 1027-1031.

[29] Simsek, O., Akoz, M.S, and Soydan, N.G., "Numerical validation of open channel flow over a curvilinear broad-creasted weir", Progress in computational fluid dynamics an international journal, vol. 16(6), 2016, p. 364-378.

[30] Sharif, N., and Rostami, A., "Experimental and numerical study of the effect of flow sepration on dissipating energy in compound bucket", APCBEE procedia, vol. 9, 2014, p. 334-338.

[31] Sparrow, E.M., Tong, J.C.K., and Abraham, J.P., "Fluid flow in a system with separate laminar and turbulent zones", Numerical Heat Transfer A, vol. 53(4), 2008, p. 341-353.

[32] Sparrow, E.M., Gorman, J.M., Abraham, J.P., and Minkowycz, W.J., "Validation of turbulence models for numerical simulation of fluid flow and convective heat transfers", Advances in Heat Transfer, vol. 49, 2017, p. 397-421.

[33] Wagner, W.E., "Hydraulic model studies of the check intake structure-potholes East canal", Bureau of reclamation hydraulic laboratory report hyd, 1956, 411.